Title

The Mitochondrial Calcium Uniporter Matches Energetic Supply with Cardiac Workload during Stress and Modulates Permeability Transition

Journal

Cell Reports, 12(1)

ISSN

2639-1856

Authors

Luongo, Timothy S
Lambert, Jonathan P
Yuan, Ancai
et al.

Publication Date

2015-07-01

DOI

10.1016/j.celrep.2015.06.017

Peer reviewed

HHS Public Access

Author manuscript

Cell Rep. Author manuscript; available in PMC 2016 July 07.

Published in final edited form as:

Cell Rep. 2015 July 7; 12(1): 23–34. doi:10.1016/j.celrep.2015.06.017.

The Mitochondrial Calcium Uniporter Matches Energetic Supply with Cardiac Workload during Stress and Modulates Permeability Transition

Timothy S. Luongo[1], **Jonathan P. Lambert**[1], **Ancai Yuan**[1], **Xueqian Zhang**[1], **Polina Gross**[3], **Jianliang Song**[1], **Santhanam Shanmughapriya**[1], **Erhe Gao**[1], **Mohit Jain**[2], **Steven R. Houser**[3], **Walter J. Koch**[1], **Joseph Y. Cheung**[1], **Muniswamy Madesh**[1], and **John W. Elrod**[1]

[1]Center for Translational Medicine, Department of Pharmacology, Temple University School of Medicine, Philadelphia, PA 19140

[2]Department of Pharmacology, University of California, San Diego, La Jolla, CA 92093

[3]Center for Cardiovascular Research, Department of Physiology, Temple University School of Medicine, Philadelphia, PA 19140

SUMMARY

Cardiac contractility is mediated by variable flux in intracellular calcium (Ca^{2+}), thought to be integrated into mitochondria via the mitochondrial calcium uniporter (MCU) channel to match energetic demand. Here we examine a conditional, cardiomyocyte-specific, mutant mouse lacking *Mcu*, the pore-forming subunit of the MCU channel, in adulthood. $Mcu^{-/-}$ mice display no overt baseline phenotype and are protected against $_{m}Ca^{2+}$-overload in an *in vivo* myocardial ischemia-reperfusion injury model by preventing the activation of the mitochondrial permeability transition pore, decreasing infarct size, and preserving cardiac function. In addition, we find that $Mcu^{-/-}$ mice lack contractile responsiveness to acute β-adrenergic receptor stimulation and in parallel are unable to activate mitochondrial dehydrogenases and display reduced bioenergetic reserve capacity. These results support the hypothesis that MCU may be dispensable for homeostatic cardiac function but required to modulate Ca^{2+}-dependent metabolism during acute stress.

Graphical Abstract

Correspondence: John W. Elrod, PhD, Center for Translational Medicine, Department of Pharmacology, 3500 N Broad St, MERB 949, Philadelphia, PA 19140, Office: (215) 707-5480, Lab: (215) 707-9144, Fax: (215) 707-9890, elrodlab.org.

Conflict of interest: The authors have no financial conflict of interest to report.

AUTHOR CONTRIBUTIONS

JWE and TSL wrote the manuscript; JWE, TSL, JPL, AY, XZ, PG, JS, SS, EG, CG, and MJ performed experiments; SRH, WJK, JYC, provided experimental oversight; JWE and MM designed experiments and JWE, MM, and SRH interpreted data.

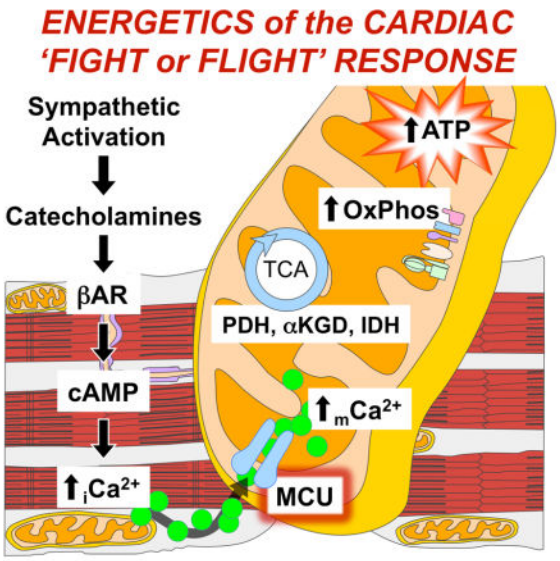

INTRODUCTION

The cardiomyocyte is unique in that a large and variable flux of intracellular ($_{i}Ca^{+2}$) must occur to mediate and regulate contraction. Thus, a complex system has evolved to regulate $_{i}Ca^{2+}$ transport to maintain homeostatic conditions (Bers, 2008). Numerous genetic components have been shown to mediate the passage of $_{i}Ca^{2+}$ across the sarcolemma and sarcoplasmic reticulum (SR) and while great strides have been made toward understanding the temporal and spatial relationship of Ca^{2+} in regards to excitation-contraction (EC) coupling, our understanding of other sub-cellular Ca^{2+} domains, including the components of mitochondria Ca^{2+} ($_{m}Ca^{2+}$) exchange remains elementary.

The dynamic Ca^{2+} environment of the heart requires that cardiac mitochondria possess an exchange system capable of dealing with the variable changes in Ca^{2+} load. Ca^{2+} enters the mitochondrial matrix via the mitochondria calcium uniporter (MCU). The MCU is an inward rectifying, low-affinity, high-capacity channel whose uptake is mediated by mitochondrial membrane potential ($\Delta\psi$ = ~ −180mV) generated by the electron transport chain (ETC) (Kirichok et al., 2004). The recent identification of the gene encoding the channel-forming portion of the uniporter, formerly named *CCDC109A* now known as *MCU*, has opened the field to genetic gain- and loss-of-function studies to determine experimentally the true role of $_{m}Ca^{2+}$ signaling in the regulation of numerous proposed cellular processes (Baughman et al., 2011; De Stefani et al., 2011). To date, multiple reports have confirmed MCU as being required for acute $_{m}Ca^{2+}$ influx into the matrix. However, numerous outstanding questions remain in regards to the molecular regulation of the MCU and the physiological function of $_{m}Ca^{2+}$, particularly in excitable cells such as cardiomyocytes.

The high metabolic demand of contractility makes it essential that an efficient and tightly controlled system be in place to regulate energy production. Oxidative Phosphorylation (OxPhos) is the largest contributor to myocardial metabolism and as such the mitochondria

represents a central control point to ensure that energy demands are met. Simultaneous measurements of $_{m}Ca^{2+}$ and NADH have correlated increased $_{m}Ca^{2+}$ load with increased oxidative phosphorylation and ATP production (Brandes and Bers, 2002; Unitt et al., 1989). Thus, Ca^{2+} is proposed to be the link between EC-coupling (ECC) and OxPhos and has been shown to modulate mitochondrial metabolism through numerous mechanisms including the activation of Ca^{2+}-dependent dehydrogenases and modulation of ETC complexes (Glancy and Balaban, 2012).

In contrast to the aforementioned pro-survival metabolic signaling, numerous studies have implicated $_{m}Ca^{2+}$ overload in the activation of apoptosis and necrosis (Rasola and Bernardi, 2011). $_{m}Ca^{2+}$ is known to cause outer-mitochondrial membrane (OMM) permeability prompting the release of apoptogens. Ca^{2+} is also thought to be the major priming event in the opening of the mitochondrial permeability transition pore (MPTP) causing the collapse of $\Delta\psi$ and loss of ATP production resulting in necrotic cell death. This mechanism of cellular demise is believed to significantly contribute to the initiation and progression of myocardial infarction and heart failure (Foo et al., 2005). In addition, it has been speculated that mitochondria in close contact to the sarcoplasmic reticulum (SR) may buffer $_{i}Ca^{2+}$ cycling and thereby play a direct role in modulating EC-coupling, providing yet another layer of potential regulation (Drago et al., 2012; Rizzuto et al., 1998).

To begin to unravel how $_{m}Ca^{2+}$ signaling modulates *in vivo* physiology a group at the NHLBI recently generated a *Mcu* gene-trap mouse (Pan et al., 2013). As expected, mitochondria isolated from this global *Mcu*-null mouse failed to take up Ca^{2+}. However, while they did find alterations in some aspects of skeletal muscle work capacity they did not find a significant cardiac phenotype. Particularly intriguing, they found no change in myocardial infarct size in an *ex vivo* global ischemia model even though *in vitro* indices of MPTP opening appeared to be completely absent. These surprising results have spurred the field to question the true role of $_{m}Ca^{2+}$ signaling in the normal and diseased heart.

To advance our understanding of $_{m}Ca^{2+}$ uptake in the heart, **in collaboration with the Molkentin Lab**, we generated a conditional, loss-of-function mouse model ($Mcu^{fl/fl}$) and coupled with a tamoxifen-inducible, cardiomyocyte-specific Cre recombinase transgenic line, deleted *Mcu* in adulthood (**REF Molkentin Cell Reports**). Here we report that loss of *Mcu* ablates $_{m}Ca^{2+}$ uptake and activity (I_{MCU}) and protects against cell death in an *in vivo* ischemia-reperfusion (IR) injury model by preventing the activation of the mitochondrial permeability transition pore (MPTP). In addition, we found that *Mcu*-null mice lacked *in vivo* contractile responsiveness to β-adrenergic receptor (βAR) stimulation and in parallel were unable to activate mitochondrial dehydrogenases and meet energetic demand. Further experimental analysis confirmed a lack of energetic responsiveness to acute sympathetic stress, supporting the hypothesis that the physiological function of the MCU is to match Ca^{2+}-dependent contractile demands with mitochondrial metabolism during the ‘fight or flight’ response.

RESULTS

Generation of a *Mcu* conditional knockout mouse model and validation of functionality

The *Mcu* targeting construct was designed with loxP sites flanking the critical exons 5-6, which encode the DIME motif, an evolutionarily conserved sequence hypothesized to be necessary for Ca^{2+} transport (Bick et al., 2012, REF TO MOLKENTIN PAPER). Three independent mutant ES cell lines were confirmed and subjected to morula aggregation and subsequent embryos transplanted into pseudo-pregnant females. Two of the three mutant ES cell lines produced germline mutant mice, which were crossed with ROSA26-FLPe mice for removal of the FRT-flanked neomycin cassette (Fig 1A). Cre-mediated deletion of exons 5-6 results in a frameshift and early termination of translation causing complete loss of MCU protein in all cells expressing Cre-recombinase. Homozygous 'floxed' mice ($Mcu^{fl/fl}$) were interbred and mouse embryonic fibroblasts (MEFs) were isolated from E13.5 embryos. MEFs were infected with adenovirus expressing Cre-recombinase (Ad-Cre) or βgal control virus and cells were lysed for Western blot analysis of MCU protein expression 6d later. Ad-Cre treatment resulted in a dose-dependent loss of MCU (Fig 1B). COXIV was used as a mitochondrial loading control. (Expression of additional $_{m}Ca^{2+}$ exchange associated proteins can be seen in Fig S1A–B.) MEFs were also examined for changes in the expression of other candidate $_{m}Ca^{2+}$ exchangers (FigS1A). ETC complex expression served as a mito loading control (Fig S1B). $Mcu^{fl/fl}$ Ad-Cre or Ad-βgal treated MEFs were subsequently infected with AAV-mitycam (mito-targeted genetic Ca^{2+} sensor) and cells imaged 48h later to monitor $_{m}Ca^{2+}$ exchange. ATP treatment (purinergic, IP3-mediated Ca^{2+} release) elicited a rapid decrease in mitycam fluorescent signal in $Mcu^{fl/fl}$ Ad-βgal MEFs (mitycam is an inverse reporter, data shown as $1\text{-}F/F_0$). Cells treated with Ad-Cre displayed almost complete loss of the acute $_{m}Ca^{2+}$ transient (Fig 1C). This difference was not attributable to a decrease in the $_{i}$Ca2+ transient (Fig S1C). Quantification of mitycam amplitude immediately following ATP treatment found a ~75% decrease in $_{m}Ca^{2+}$ (Fig 1D). It should be noted that we did consistently observe that Mcu-KO MEFs continued to slowly take up Ca^{2+} and eventually reached levels equivalent to control cells. Next, $Mcu^{fl/fl}$ Ad-Cre or Ad-βgal infected MEFs were examined for $_{m}Ca^{2+}$ uptake capacity by loading digitonin permeabilized cells with the Ca^{2+} sensor, Fura-FF, and the membrane potential sensitive dye, JC-1 for simultaneous ratiometric recording. Cells were treated with thapsigargin to inhibit SERCA and block ER Ca^{2+} uptake. Upon reaching a steady-state membrane potential cells were exposed to seven consecutive pulses of 5-μM Ca^{2+} (Fig 1E–F). A decrease in Fura signal after each bolus of bath Ca^{2+} represents $_{m}Ca^{2+}$ uptake. Quantitative analysis after exposure to 10-μM Ca^{2+} (a concentration where MCU is fully activated in non-excitable cells) revealed *Mcu-null* MEFs to have a near complete loss of $_{m}Ca^{2+}$ uptake compared to control MEFs (Fig 1G). Analysis of $\Delta\psi$ revealed no difference between groups at baseline or after delivery of 10-μM Ca^{2+}, confirming the observed change in uptake was not a result of an alteration in the driving force for $_{m}Ca^{2+}$ uptake (Fig 1H). Incremental increases in $_{m}Ca^{2+}$ eventually led to a decrease in membrane potential in βgal control MEFs, a phenomenon not observed in *Mcu-null* MEFs even after substantial Ca^{2+} challenge (Fig 1I). It should be noted that in an attempt to make a MEF $Mcu^{-/-}$ cell line we crossed $Mcu^{fl/fl}$ mice with a trangenic germline-Cre model (B6.CMV-Cre, JAX Mice) to generate $Mcu^{+/-}$

for subsequent interbreeding. However, heterozygous mating (>6 litters) failed to yield *Mcu*$^{-/-}$ pups, suggesting homozygous deletion results in embryonic lethality.

Genetic deletion of Mcu results in the complete loss of uniporter Ca^{2+} uptake in ACMs

Mcu$^{fl/fl}$ mice were crossed with the well-characterized αMHC-Cre transgenic mouse model to yield cardiomyocyte-specific loss of *Mcu* (Fig 2A). Adult cardiomyocytes (ACMs) were isolated from wild-type (WT), αMHC-Cre, *Mcu*$^{fl/fl}$ and *Mcu*$^{fl/fl}$ x αMHC-Cre mice at 8–12 wks of age. Western blot assessment found a ~80% reduction in MCU protein compared to all controls; in accordance with previous reports of the mosaicism of the αMHC-Cre transgenic strain (Fig 2B) (Oka et al., 2006). No expression changes in ETC complex subunits were found (Fig S2A). To examine baseline $_{m}Ca^{2+}$ content ACMs were loaded with the ratiometric Ca^{2+} reporter, Fura-2, and treated with Ru360 (MCU inhibitor), CGP37157 ($_{m}$NCX inhibitor), thapsigargin (SERCA inhibitor) and permeabilized with digitonin to block all Ca^{2+} flux. During spectrofluorometric recording the protonophore, FCCP, was injected to dissipate Δψ allowing the release of all matrix free-Ca^{2+} (Fig 2C). Quantification of these data by calibration of the Fura-2 reporter in our experimental system (Fig S2B) found no change in matrix Ca^{2+} content in *Mcu* knockout (KO) ACMs (Fig 2D). Next, $_{m}Ca^{2+}$ uptake capacity was evaluated in ACMs isolated from both *Mcu*$^{fl/fl}$ and *Mcu*$^{fl/fl}$ x αMHC-Cre mice (Fig 2E–F). The simultaneous recording of $_{m}Ca^{2+}$ uptake and membrane potential discovered that *Mcu KO* ACMs were completely refractory from high Ca^{2+} challenge and failed to take up Ca^{2+}, quantified after the second 10-μM Ca^{2+} pulse (Fig 2G). *Mcu*$^{fl/fl}$ x αMHC-Cre ACMs displayed a slightly higher baseline mitochondrial membrane potential, although not reaching statistical significance, confirming that the lack of Ca^{2+} uptake was not due to a decrease in Δψ (Fig 2H). Further, *Mcu-null* ACMs were entirely resistance to Ca^{2+}-overload loss of Δψ as observed in control cells. In fact, nine repeated boluses of 10-μM Ca^{2+} failed to elicit mitochondrial depolarization in *Mcu* KO ACMs (Fig 2I).

To confirm that deletion of the *Mcu* gene results in loss of MCU channel activity (I_{MCU}), we isolated ACM's, generated mitoplasts, and employed the whole-mitoplast voltage-clamping technique developed by the Clapham group that first established the uniporter as the prototypical uptake channel (Kirichok et al., 2004). I_{MCU} was absent in *Mcu-null* mitoplasts subjected to a ramping protocol from −160 mV to 80 mV (Fig 2J). Quantitative analysis revealed a decrease in current density (Fig 2K) and likewise the current-time integral (area under the curve) was minimal (Fig 2L). These data are in agreement with initial and subsequent reports of MCU channel biophysical activity (Chaudhuri et al., 2013; Fieni et al., 2012; Kirichok et al., 2004). Collectively, these experiments corroborate that *Mcu* is necessary for rapid $_{m}Ca^{2+}$ uptake in cardiomyocytes.

Mcu-mediated $_{m}Ca^{2+}$ uptake is a significant contributor to myocardial IR-injury

Given the well-substantiated role of Ca^{2+} in activating the MPTP and the numerous reports that MPTP inhibition is a potent therapeutic strategy to reduce necrotic cell death (Rasola and Bernardi, 2011) we next assessed genetic loss of *Mcu* in an *in vivo* model of myocardial IR-injury. *Mcu*$^{fl/fl}$, αMHC-MerCreMer (MCM), and *Mcu*$^{fl/fl}$ x αMHC-MCM (*Mcu* cKO) mice (age 10–12 wks) were all injected i.p. for 5 consecutive days with 40 mg/kg tamoxifen

(see Fig S3A–B *for $_{m}Ca^{2+}$ exchange associated proteins and ETC complex expression post-tamoxifen)* and 3wks later subjected to left coronary artery (LCA) ligation for 40m and 24h reperfusion (Fig 3A). The evaluation of LV infarct size by TTC staining and Evan's blue dye perfusion revealed *Mcu* cKO mice to have a ~45% reduction in infarct size (INF) per area-at-risk (AAR) vs. controls; AAR was similar between all groups (Fig 3B–C). To corroborate this result serum from the same cohort of mice was collected 24h after reperfusion and a cardiac troponin-I (cTnI) ELISA was performed as a secondary marker of cardiomyocyte cell death. *Mcu* deleted mice displayed a ~65% reduction in cTnI vs. controls (Fig 3D). We also examined DNA fragmentation by TUNEL staining, to demarcate cell death. We found a significant reduction in TUNEL+ nuclei in the infarct boarder zone of *Mcu* cKO hearts as compared to controls (Fig S3C–D).

Echocardiographic assessment of LV function 24h post-IR revealed a significant preservation of LV end-systolic diameter (LVESD) and percent fractional shortening (FS%) in *Mcu* knockout mice (Fig 3E–G). Additional M-mode echocardiographic data can be seen in Table S1. To account for differences in regional wall motion due to variances in infarct size we utilized speckle-tracking of B-mode echocardiographic recordings and likewise found an improvement in LV function in *Mcu* cKO mice post-IR (Fig S3E–I).

To further examine the resistance of *Mcu-null* cardiomyocytes to mitochondrial depolarization during Ca^{2+}-overload as reported above in Fig 2I; we next isolated mitochondria from hearts and employed the classical mitochondrial-swelling assay to examine MPTP opening. Mitochondria isolated from *Mcu*-KO hearts failed to swell in response to increasing bath Ca^{2+}, signified by a decrease in absorbance, in striking contrast to control mitochondria (Fig 3H, red vs. black line). For these experiments we utilized a substantial Ca^{2+} bolus (500-μM), such that the CypD inhibitor cyclosporine A (CsA) only had a partial inhibitory effect on swelling (grey line) in comparison to *Mcu* deletion. These data are quantified in Fig 3I as percent change in area-under- the-curve vs. control. It has previously been reported that MPTP opening occurs independent of CypD at high Ca^{2+} loads similar to those utilized here (Baines et al., 2005). To account for possible compensatory alterations in the expression of MPTP components, we immunobloted for CypD, ANT, and VDAC (Fig S3J). We found no differences in expression between *Mcu* cKO and control hearts. These results support the hypothesis that the loss of *Mcu* prevents Ca^{2+} from entering the matrix and activating the MPTP and thereby reduces IR-mediated cardiomyocyte cell death.

$_{m}Ca^{2+}$ uptake is necessary to match energetic supply with β-adrenergic contractile demand

Numerous studies have suggested that ECC Ca^{2+} cycling is integrated into mitochondria to match ATP production with workload (Williams et al., 2015). Given that we did not find a significant difference in baseline cardiac function or resting $_{m}Ca^{2+}$ content, we next induced acute cardiac stress using an adrenergic agonist to elevate the $_{i}Ca^{2+}$ load in an attempt to unmask the physiological function of the MCU. *Mcu$^{fl/fl}$*, αMHC-MCM, and *Mcu* cKO mice were injected i.p. for 5 consecutive days with 40 mg/kg tamoxifen and 10d later we measured LV hemodynamic parameters during i.v. infusion of isoproterenol (Iso) (Fig 4A).

Mcu cKO mice failed to increase LV contractility (dp/dt max) in response to β-adrenergic stimulation as compared to control mice (Fig 4B). In addition there was a noted, although less dramatic, impairment in LV relaxation (dp/dt min, Fig 4C). There was no significant difference in heart rate (HR) between groups over the course of Iso infusion (Fig 4D).

Following 10m of Iso-infusion, we snap-froze ventricular tissue for metabolic analysis. We first evaluated the status of the pyruvate dehydrogenase complex (PDH), the prototypical $_{m}Ca^{2+}$- dependent enzyme that converts pyruvate into acetyl-CoA for use in the tricarboxylic acid (TCA) cycle. PDH is a central component linking glycolysis to OxPhos and also a contributor to the NADH pool. $_{m}Ca^{2+}$ is reported to increase PDH phosphatase activity (*PDP1*), which in turn dephosphorylates the S293 residue on the E1 subunit resulting in increased PDH enzymatic activity. There was no change in the baseline expression of phospho-PDH, total PDH complex (Fig 4E), or other proposed $_{m}Ca^{2+}$-regulated dehydrogenases (α-ketoglutarate dehydrogenase and isocitrate dehydrogenase (Fig S4A). However, expression analysis of post-Iso samples revealed a substantial decrease in phosphorylation of S293-E1 in control hearts vs. *Mcu* cKO samples (Fig 4F, top panel). There was no change in total protein expression for any of the PDH subunits post-Iso (Fig 4F, bottom panel). Quantification of phospho/total E1-PDH revealed *Mcu-KO* hearts to have greater than a 3-fold difference in phosphorylation vs. controls, signifying a failure to activate PDH during adrenergic stimulation (Fig 4G). This result was confirmed by our observation of a ~50% decrease in Iso-stimulated PDH enzymatic activity in *Mcu* cKO hearts (Fig 4H and Fig S4B). To examine baseline energetics in more detail and rule out any compensatory changes in our *Mcu* cKO model we employed metabolomics to measure the levels of several prominent TCA intermediates (Fig S4C–D). Mass spectrometry of ventricular tissue found no difference in any of the metabolites assayed.

Next, we measured the NAD^{+}/NADH ratio and while we found no difference at baseline, acute Iso stimulation revealed a ~2-fold difference in *Mcu* cKO hearts vs. controls (Fig 4I). We also examined the $NADP^{+}$/NADPH ratio and again found no difference at baseline but did find a trend of increased $NADP^{+}$/NADPH ratio in *Mcu* cKO hearts during Iso-infusion (Fig S4E). This was a somewhat surprising since we thought NADPH generation was primarily extra-mitochondrial via the pentose phosphate pathway. However, mitochondrial enzymes such as malic enzyme, NADP-linked isocitrate dehydrogenase and mitochondrial methylenetetrahydrofolate dehydrogenase are other significant sources of NADPH production (Fan et al., 2014; Huang and Colman, 2005; Palmieri et al., 2015; Yang et al., 1996). It's intriguing to think that this may be another metabolic consequence of altering the $_{m}Ca^{2+}$microdomain during stress, be it direct or indirect modulation.

To further examine the hypothesis that *Mcu*-Ca^{2+} uptake is necessary to increase myocardial energy production in response to acute sympathetic signaling we employed a cellular system to monitor energetic changes in real-time. ACMs were isolated from $Mcu^{fl/fl}$ and $Mcu^{fl/fl}$ x αMHC-MCM mice 10d after administration of tamoxifen. We first monitored $_{i}Ca^{2+}$ transients at both baseline and during Iso-delivery to rule out the possibility of decreased βAR-responsiveness in our *Mcu* cKO cells (Fig S5). We found *Mcu* cKO ACMs to have no impairment in Iso-mediated augmentation of $_{i}Ca2+$ signaling during pacing. Next, ACMs were monitored for changes in NADH autofluorescence intensity (Fig 5A). While we found

no difference in basal NADH levels between groups (Fig 5B), the administration of Iso (10-μM) elicited a significant increase in NADH production in control ACMs, while *Mcu*-KO myocytes were unresponsive with NADH consumption being greater than production. Quantification of this data with correction to control ACMs can be seen in Fig 5C. To examine maximal NADH production in the presence of Iso we next inhibited complex I of the ETC (NADH dehydrogenase) with rotenone. *Mcu*-KO ACMs displayed a ~50% reduction in maximal NADH production, as compared to control (Fig 5D). To evaluate if the lack of NADH-responsiveness correlated with an alteration in OxPhos capacity we measured ACM oxygen consumption rates (OCR) using a Seahorse extracellular flux analyzer. Corroborating our previous data showing no change in baseline NADH, there was no difference in baseline respiration between groups (Fig 5E). Next, we examined maximal respiratory capacity ($_{max}$OCR, FCCP treatment) in the presence of Iso or vehicle (veh). *Mcu-null* ACMs displayed a significant reduction in $_{max}$OCR, as compared to controls, and were completely refractory to Iso-mediated increases in mitochondrial respiration (Fig 5F). In summation, these results support the concept of metabolic failure due to an inability to increase reducing equivalents during acute stress.

DISCUSSION

Since the 1970's it was apparent that mitochondria contained a protein capable of inducing an inward rectifying Ca^{2+} current (Sottocasa et al., 1972). The subsequent identification of a pharmacological inhibitor, of the channel, ruthenium red (RR), allowed investigators to begin to probe the cellular function of $_{m}Ca^{2+}$ exchange (Moore, 1971). Various studies employing RR or a derivative have implicated $_{m}Ca^{2+}$ in numerous cellular processes, most notably the regulation of metabolism, cell death, and buffering of cytosolic Ca^{2+} signaling (Hoppe, 2010). However, subsequent studies have found a multitude of cation channels that are inhibited by RR derivatives. Thus, off-target effects of these pharmacological agents may account for the conflicting results that have fueled the debate as to the true biological function of this microdomain. Further impeding causative experimentation was the unknown genetic identity of the constituents that comprise the $_{m}Ca^{2+}$ exchange machinery. Reports from two independent laboratories identified *MCU* as the channel-forming component of the MCU complex and documented its requirement for Ca^{2+} uptake (Baughman et al., 2011; De Stefani et al., 2011). With this discovery the race was on to generate a loss-of-function mouse model for comprehensive study to begin to put into context the vast and often controversial literature regarding how the dynamic flux of Ca^{2+} into and out of the mitochondrial matrix may regulate (patho)physiology. A recent report from Pan et al. details the phenotype of a *Mcu*-null mouse generated using a gene trap strategy (Pan et al., 2013). While the authors reported a complete loss acute $_{m}Ca^{2+}$ uptake in various cell types, the physiological results of the study were quite surprising. Perhaps most striking was that *Mcu* ablation had little effect on cardiac function, structure or cell death. These results have prompted the field at large to question the relevance of cardiomyocyte $_{m}Ca^{2+}$ flux. Beyond this report, a number of other questions remained unresolved regarding the impact of $_{m}Ca^{2+}$ signaling in cardiomyocyte function.

Using a conditional knockout approach to specifically delete *Mcu* in cardiomyoyctes in adult mice coupled with *in vivo* experimental methodologies we were able to document how

acute $_{m}Ca^{2+}$ uptake impacts cardiac physiology. We found: 1) a reduction in infarct size assessed both histologically by TTC-staining and TUNEL and biochemically by cTnI levels coupled with *in vivo* LV functional data, that all support the notion that *Mcu*-mediated $_{m}Ca^{2+}$ uptake contributes to IR-induced cardiomyocyte cell death; 2) that *Mcu* KO cells displayed a greater resistance to Ca^{2+}-overload, capable of maintaining $\Delta\psi$ following numerous pulses of Ca^{2+} in contrast to control cells; 3) that cardiac mitochondria isolated from *Mcu*-null cardiomyocytes were completely resistant to swelling. Together these data suggest deletion of *Mcu* greatly decreases susceptibility to MPTP activation and thereby provides protection against necrotic cell death. This result is not surprising given the numerous reports implicating $_{m}Ca^{2+}$ load as a fundamental contributor to MPTP open probability (Rasola and Bernardi, 2011). Moreover, studies have shown that MPTP inhibition is potently cytoprotective, particularly in I/R-injury, including a clinical trial evaluating the efficacy of cyclosporine-A (MPTP inhibitor) administration during reperfusion of the ischemic myocardium (Elrod and Molkentin, 2013; Piot et al., 2008). It is likely that MPTP inhibition was not the sole protective mechanism, as decreasing $_{m}Ca^{2+}$ load is also associated with decreased ROS generation during stress. Supporting this concept we found a significant decrease in mitochondrial superoxide levels in *Mcu*-null cells following hypoxia/reoxygenation (Fig S1D–E).

However, our IR-injury results are contradictory to those recently reported by Pan et al. (Pan et al., 2013). Disparities in methodology likely account for the different results observed here. The previous study used a gene-trap approach with germline gene inactivation, versus our conditional, cardiomyocyte-specific deletion in the adult mouse. Therefore, compensatory pathways, induced by the loss of *Mcu* during development, may have allowed for the entry of Ca^{2+} into the matrix in sufficient quantity, independent of MCU, to activate mitochondrial-dependent death pathways or alternatively mitochondrial-independent cell death pathways may be upregulated in this mouse. Our finding that germline deletion of *Mcu* in our model system was embryonically lethal, while knocking-out *Mcu* after birth or in adulthood resulted in no discernable baseline phenotype supports the notion that significant gene changes must have occurred prenatally in their model to support viability. Further, it may be that deletion of *Mcu* in other cell types in the heart, such as fibroblasts and endothelial cells, actually magnified injury by reducing the $_{m}Ca^{2+}$-buffering capacity in non-myocytes and thereby masked the protective effect of loss of *Mcu* in cardiomyocytes. Supporting this concept we found that *Mcu*-null MEFs displayed an increase in $_{i}Ca^{2+}$ transient amplitude following IP3R stimulation (Fig. S1C). Yet another possible reason is the disparity in ischemic models. The Pan et al. study employed an *ex vivo* Langendorff global hypoxia model compared to our *in vivo* LCA ligation IR model. There are major differences between these methodologies and while unlikely, perhaps the *ex vivo* model somehow lessens the contribution of MCU-dependent Ca^{2+} uptake in cardiomyocyte death. Our data do fit with previous reports of ruthenium red derivatives (MCU inhibitors) providing protection against IR-injury (Zhang et al., 2006; Zhao et al., 2013).

The other major difference from the Pan et al. study is that we found no change in resting $_{m}Ca^{2+}$ content in *Mcu* null cells, in contrast to their finding of ~70% reduction in skeletal muscle $_{m}Ca^{2+}$. Our results suggest a MCU-independent mechanism of $_{m}Ca^{2+}$

uptake is a significant contributor to homeostatic $_{m}Ca^{2+}$ levels. We hypothesize that the threshold for MCU-mediated Ca^{2+} entry is not reached under homeostatic conditions in adult cardiomyocytes and that an alternative slow $_{m}Ca^{2+}$ uptake mechanism must play a significant role. Direct evidence that *Mcu*-independent $_{m}Ca^{2+}$ uptake exists can be seen in our experiment examining real-time flux in MEFs (Fig 1C). Although we observed complete loss of the acute and rapid MCU-like $_{m}Ca^{2+}$ uptake, $_{m}Ca^{2+}$ content continued to slowly rise with sustained $_{i}Ca^{2+}$ load and eventually reached a level equivalent to WT cells. It's possible that the lower $_{m}Ca^{2+}$ content previously reported in Pan et al. can be explained by methodological differences. We discovered that the slightest perturbation in either extracellular or $_{i}Ca^{2+}$ stores in WT cells induced an increase in $_{m}Ca^{2+}$ loading. We found that any Ca^{2+} liberated during our experimental procedure, be it from mitochondrial isolation or SERCA inhibition, was immediately taken up by WT mitochondria in a *Mcu*-dependent fashion. Therefore such a perturbation elevates $_{m}Ca^{2+}$ content in control cells and may lead to a false interpretation of decreased content in *Mcu* KO cells. This phenomenon can be seen in Fig S2C where in control cells after permeabilization and addition of thapsigargin we see a decrease in the Fura ratio prior to FCCP treatment signifying $_{m}Ca^{2+}$ uptake; whereas in *Mcu*-deleted cells we observe a rise in extra-mitochondrial Ca^{2+} levels. The addition of the MCU inhibitor, Ru360, and $_{m}$NCX inhibitor, CGP37157, prior to experimentation alleviated this problem. Summarizing the first part of our study, in a clinically relevant model of IR-injury we provide evidence that *Mcu*-mediated Ca^{2+} uptake is a significant mechanism driving MPTP-mediated cardiomyocyte cell death and cardiac dysfunction. Further, we hypothesize that the $_{m}Ca^{2+}$ exchange system possess a great deal of plasticity and that alternative uptake mechanisms maintain matrix Ca^{2+} content during homeostasis. A more detailed examination of this phenomenon in future studies may aid the discovery of novel exchangers and pathways that account for the observed "slow $_{m}Ca^{2+}$ uptake".

The heart is an aerobic organ that must constantly match energy supply with demand. The contractile function of the normal heart changes significantly during normal activities. This has led to the theory that $_{i}Ca^{2+}$ cycling is integrated with mitochondria on a beat-to-beat basis to match ATP production with contractile demand as a real-time regulator of oxidative metabolism (Glancy and Balaban, 2012). However, our current findings suggest that rapid MCU-dependent Ca^{2+} uptake is dispensable for homeostatic cardiac function, as ablating *Mcu* had little effect on baseline function for all measured indices, including little to no change in LV function, structure and cellular energetics. We found cardiomyocyte resting $_{m}Ca^{2+}$ content to be ~200 nM and we did not detect appreciable mitochondrial uptake until concentrations of ~8-μM were reached (control ACMs displayed only ~17% uptake in response to a 10-μM Ca^{2+} load). Both of these values fit nicely within the range of previous studies examining cardiac MCU function that were recently summarized in eloquent fashion by Lederer and colleagues (Williams et al., 2013). These data also agree with recent work proposing MICU1 binds MCU to inhibit uptake until a given threshold or set-point of Ca^{2+} is overcome (Csordas et al., 2013; Mallilankaraman et al., 2012). Since it is assumed global ECC $_{i}Ca^{2+}$ cycling does not reach such levels in the homeostatic beating heart we hypothesize that a slow MCU-independent influx mechanism must account for homeostatic maintenance of matrix Ca^{2+}, aided by balanced $_{m}$NCX efflux rates. It should be

noted that Ca^{2+} levels of this magnitude might occur in discrete microdomains where a sub-population of mitochondria are tethered in close proximity to SR/T-tubule junctions (Chen et al., 2012). There are a number of mechanisms that theoretically could contribute to a slow MCU-independent $_{m}Ca^{2+}$ uptake including: $_{mito}$RyR, LETM1 (H^{+}/Ca^{2+} exchanger), reverse-mode $_{m}$NCX, or an as of yet unknown exchanger(s) (Beutner et al., 2001; Jiang et al., 2009; Palty et al., 2010). Additional evidence supporting MCU-independent uptake can be seen in a recent biophysical report describing a second 'RR-insensitive' voltage dependent inward rectifying current (Michels et al., 2009). We hope that our future experiments will aid the identification of this MCU-independent uptake mechanism.

While our data do not support a significant role for the MCU in basal cardiac physiology, cardiomyocyte-specific deletion did result in a striking inability to increase contractile function in response to the classic β-agonist, isoproterenol. Since a study published by Howell and Duke in 1906, it has been appreciated that Ca^{2+} is required for the "augmenting influence of the sympathetic upon the heart (Howell and Duke, 1906)." Our understanding has continued to evolve over the last century and the various molecular mechanisms of how βAR signaling regulates changes in excitation-contraction-coupling (ECC) have been defined (Bers, 2008). Our data extend these pathways to include MCU-dependent Ca^{2+} uptake as a mechanism necessary to upregulate energetics to support increases in cardiac contractility during acute sympathetic stress. Catecholamine signaling as occurs with the 'fight or flight' response, strenuous exercise, or in the failing heart, elicits a marked increase in $_{i}Ca^{2+}$ levels. Specifically, isoproterenol has been shown to dramatically increase peak $_{i}Ca^{2+}$ and SR Ca^{2+} load/release to levels sufficiently beyond those we show here are required for MCU-dependent uptake (Curran et al., 2007). This large increase in $_{i}Ca^{2+}$ is integrated into mitochondria to directly impact cellular energetics at multiple control points. $_{m}Ca^{2+}$ increases the activity of three matrix dehydrogenases that are rate-limiting in the tricarboxylic (TCA) cycle (Denton, 2009). Most notably, matrix Ca^{2+} has been shown to indirectly activate pyruvate dehydrogenase (PDH), which converts pyruvate to acetyl-CoA for entry into the TCA cycle and as such also links glycolysis with OxPhos (McCormack and England, 1983). We found a marked decrease in PDH E1 phosphorylation following Iso treatment in control cells, indicative of increased $_{m}Ca^{2+}$- dependent phosphatase activity and subsequent PDH enzymatic activation. In contrast, dephosphorylation of PDH was completely lacking in *Mcu*-KO hearts and PDH activity during isoproterenol administration was reduced by ~50%. In both *in vivo* and *in vitro* experiments we discovered that loss of *Mcu* ablated Iso-mediated increases in NADH and OxPhos capacity. Generally, our metabolic findings are in agreement with Pan et al., which found similar alterations in skeletal muscle metabolism and work capacity in $Mcu^{-/-}$ mice subjected to starvation (Pan et al., 2013). Similarly, our study found no change in baseline metabolic function or metabolite levels. However, our finding that HR was not altered in *Mcu* cKO mice does differ from a recent report by the Anderson group where they reported that a MCU-dominant negative mouse model lacked chronotropic responsiveness to β-adrenergic stimulation (Wu et al., 2015). This may be due to a difference in methodology, as we did not examine HR with implantable telemeters in conscious mice void of anesthesia. Overall our model does support their hypothesis of MCU-mediated Ca^{2+} entry playing a significant role in the cardiac "fight or flight" response.

In summary, we show that the physiological function of MCU-mediated Ca^{2+} uptake in the heart is to augment mitochondrial energetic signaling to match ATP production with contractile demand during periods of acute adrenergic stress. In addition, our findings support a pathological role for MCU Ca^{2+} influx driving mitochondrial depolarization and cell death during IR-injury. While much work remains to fully elucidate all the molecular constituents of the MCU complex and their mechanistic function, our current study provides a fundamental framework to aid our understanding of $_{m}Ca^{2+}$ uptake in health and disease.

EXPERIMENTAL PROCEDURES

Please see the attached Supplemental Information for detailed experimental procedures.

Generation of Mcu conditional knockout mice

The gene targeting strategy in embryonic stem cells to generate the Mcu-loxP mice that we used here is described in Kwong et al {REF: INSERT REF TO MOLKENTIN PAPER}, which is a companion paper in this same issue. In short, a *Mcu* conditional knockout mouse by recombinant insertion of a targeting gene construct containing loxP sites flanking exons 5-6 of the *Mcu* gene (ch10: 58930544-58911529) in mouse ES cells. 3 independent mutant ES cell lines were confirmed and subjected to morula aggregation and subsequent embryos transplanted into pseudo-pregnant females. 2 of the 3 mutant ES cell lines produced germline mutant mice, which were crossed with ROSA26-FLPe knock-in mice for removal of the FRT-flanked neomycin cassette. Resultant $Mcu^{fl/fl}$ mice were crossed with cardiac specific-Cre transgenic mice, αMHC-Cre and αMHC-MCM, to generate cardiomyocyte-specific *Mcu* knockouts. B6.CMV-Cre transgenic mice (Jackson Laboratory, Stock # 006054) were used for germline deletion. For temporal deletion of *Mcu* using the MCM model, $Mcu^{fl/fl}$, αMHC-MCM, and $Mcu^{fl/fl}$ x αMHC-MCM were injected i.p. 40 mg/kg/day of tamoxifien for 5 consecutive days. For all experiments mice were 10–14wks of age. All mutant lines were maintained on the C57/BL6 background and all experiments involving animals were approved by Temple University's IACUC and followed AAALAC guidelines.

Western blot analysis

All procedures were carried out as previously reported (Elrod et al., 2010).

Isolation of ACMs

ACMs were isolated from ventricular tissue as described previously (Zhou et al., 2000). All cells were used within 4h of isolation.

Evaluation of $_{m}Ca^{2+}$ uptake and content

To evaluate $_{m}Ca^{2+}$ content, permeabilized ACMs were treated with RU360 and CGP-37157 to inhibit $_{m}Ca^{2+}$ flux. Fura2 (Invitrogen) was added to monitor extra-mitochondrial Ca^{2+}. FCCP was added to uncouple the $\Delta\psi$ and release matrix free- Ca^{2+}. To measure $_{m}Ca^{2+}$ uptake capacity, ACMs were permeabilized and Fura-FF (Invitrogen) was added to monitor extra-mitochondrial Ca^{2+}. JC-1 (Enzo) was added to monitor $\Delta\psi$. Fluorescence signals for JC-1 and Fura were monitored on a PTI spectrofluorometer. All details are previously reported (Mallilankaraman et al., 2012).

Mitochondria Isolation and Swelling Assay

Hearts were excised from mice and mitochondria were isolated as reported (Frezza et al., 2007). For the swelling assay, mitochondria were diluted in assay buffer and abs recorded at 540nm every 5s. 500-μM $CaCl_2$ was injected to induce swelling +/− 2-μM Cyclosporin A (CsA) (Elrod et al., 2010).

ACM $_{i}Ca^{2+}$ transients

Isolated ACMs were loaded with Fluo-4 AM (Invitrogen) and placed in a 37°-C heated chamber on an inverted microscope stag e. ACMs were perfused with Tyrode's buffer and paced at 0.5 Hz. After baseline recordings, cells were perfused with Tyrode's containing 100-nM Iso. Ca^{2+} transients were analyzed using Clampfit software.

Mitoplast patch-clamp analysis of MCU Current

Following mitochondrial isolation, mitoplasts were prepared for patch-clamp studies. I_{MCU} was recorded as previously described in detail (Kirichok et al., 2004).

Metabolic Assays

Metabolomic analyses were carried out by metabolite profiling of ventricular tissue by LC-MS/MS as described (Jain et al., 2012). NAD/NADH and NADP/NADPH ratios were quantified using luminescence assays (Promega). PDH activity was quantified using a fluorometric assay (Mitosciences). *In vitro* experiments of ACM NADH production was monitored by recording autofluorescence using a spectrofluorometer. A XF96 extracellular flux analyzer (Seahorse Biosciences) was employed to measure OCR in isolated ACMs.

LV Echocardiography and Hemodynamics

Transthoracic echocardiography of the LV was performed and analyzed on a Vevo 2100 imaging system as previously reported (Elrod et al., 2007). Invasive hemodynamic measurements in anesthetized mice was performed using a pressure catheter inserted into the right carotid artery and guided into the LV. Right jugular vein catheterization allowed delivery of Iso during recording.

Myocardial IR-Injury

LCA ligation and reperfusion was performed as previously described in Gao et al. (Gao et al., 2010). Infarct size was measured as previously reported (Elrod et al., 2007). Serum was collected from mice after 24h R to measure cTnI using the Life Diagnostics, Inc. ELISA kit. A TUNEL detection kit (Roche) was used to label DNA fragmentation in the infarct border zone of fixed heart sections.

MEF isolation

Embryos were collected from *Mcu*$^{fl/fl}$ mice at E13.5 and MEFs isolated as previously reported (Baines et al., 2005). MEFs were treated with Ad-Cre or Ad-βgal for 24h. 6d post-infection cells were used for experiments.

$_{i}Ca^{2+}$ and $_{m}Ca^{2+}$ flux in MEFs

MEFs were infected with AAV-mitycam to measure $_{m}Ca^{2+}$ exchange or loaded with the $_{i}Ca^{2+}$ indicator, Fluo4-FF. Data was collected every 3s and analyzed on Zen software.

Hypoxia/Reoxygenation

MEFs were plated on 35mm glass plates and after culturing for 24h, loaded with 5-μM MitoSOX Red (Invitrogen). Cells were placed in ischemic medium for 1h, reoxygenated with Tyrode's buffer and imaged 5min later to evaluate mitochondrial superoxide production.

Statistics

All results are presented as mean +/− SEM. Statistical analysis was performed using Prism 6.0 software (GraphPad). Where appropriate column analyses were performed using an unpaired, 2-tailed t-test (for 2 groups) or one-way ANOVA with Bonferroni correction (for groups of 3 or more). For grouped analyses either multiple unpaired t-test with correction for multiple comparisons using the Holm-Sidak method or where appropriate 2-way ANOVA with Tukey post-hoc analysis was performed. P values less than 0.05 were considered significant.

Supplementary Material

Refer to Web version on PubMed Central for supplementary material.

Acknowledgments

The authors express thanks to Dr. Joseph Rabinowitz's lab for amplification of AAV-mitycam. This work was supported by grants to JWE from the NIH/NHLBI (HL123966), AHA (14SDG18910041), and W.W. Smith Charitable Trust (H1301), and NIH/NIDA (P01 DA037830, PI: K Khalili).

References

Baines CP, Kaiser RA, Purcell NH, Blair NS, Osinska H, Hambleton MA, Brunskill EW, Sayen MR, Gottlieb RA, Dorn GW, et al. Loss of cyclophilin D reveals a critical role for mitochondrial permeability transition in cell death. Nature. 2005; 434:658–662. [PubMed: 15800627]

Baughman JM, Perocchi F, Girgis HS, Plovanich M, Belcher-Timme CA, Sancak Y, Bao XR, Strittmatter L, Goldberger O, Bogorad RL, et al. Integrative genomics identifies MCU as an essential component of the mitochondrial calcium uniporter. Nature. 2011; 476:341–345. [PubMed: 21685886]

Bers DM. Calcium cycling and signaling in cardiac myocytes. Annual review of physiology. 2008; 70:23–49.

Beutner G, Sharma VK, Giovannucci DR, Yule DI, Sheu SS. Identification of a ryanodine receptor in rat heart mitochondria. The Journal of biological chemistry. 2001; 276:21482–21488. [PubMed: 11297554]

Bick AG, Calvo SE, Mootha VK. Evolutionary diversity of the mitochondrial calcium uniporter. Science (New York, N Y. 2012; 336:886.

Brandes R, Bers DM. Simultaneous measurements of mitochondrial NADH and Ca(2+) during increased work in intact rat heart trabeculae. Biophys J. 2002; 83:587–604. [PubMed: 12124250]

Chaudhuri D, Sancak Y, Mootha VK, Clapham DE. MCU encodes the pore conducting mitochondrial calcium currents. eLife. 2013; 2:e00704. [PubMed: 23755363]

Chen Y, Csordas G, Jowdy C, Schneider TG, Csordas N, Wang W, Liu Y, Kohlhaas M, Meiser M, Bergem S, et al. Mitofusin 2-containing mitochondrial-reticular microdomains direct rapid cardiomyocyte bioenergetic responses via interorganelle Ca(2+) crosstalk. Circulation research. 2012; 111:863–875. [PubMed: 22777004]

Csordas G, Golenar T, Seifert EL, Kamer KJ, Sancak Y, Perocchi F, Moffat C, Weaver D, de la Fuente Perez S, Bogorad R, et al. MICU1 controls both the threshold and cooperative activation of the mitochondrial Ca(2)(+) uniporter. Cell metabolism. 2013; 17:976–987. [PubMed: 23747253]

Curran J, Hinton MJ, Rios E, Bers DM, Shannon TR. Beta-adrenergic enhancement of sarcoplasmic reticulum calcium leak in cardiac myocytes is mediated by calcium/calmodulin-dependent protein kinase. Circulation research. 2007; 100:391–398. [PubMed: 17234966]

De Stefani D, Raffaello A, Teardo E, Szabo I, Rizzuto R. A forty-kilodalton protein of the inner membrane is the mitochondrial calcium uniporter. Nature. 2011; 476:336–340. [PubMed: 21685888]

Denton RM. Regulation of mitochondrial dehydrogenases by calcium ions. Biochim Biophys Acta. 2009; 1787:1309–1316. [PubMed: 19413950]

Drago I, De Stefani D, Rizzuto R, Pozzan T. Mitochondrial Ca2+ uptake contributes to buffering cytoplasmic Ca2+ peaks in cardiomyocytes. Proceedings of the National Academy of Sciences of the United States of America. 2012; 109:12986–12991. [PubMed: 22822213]

Elrod JW, Calvert JW, Morrison J, Doeller JE, Kraus DW, Tao L, Jiao X, Scalia R, Kiss L, Szabo C, et al. Hydrogen sulfide attenuates myocardial ischemia-reperfusion injury by preservation of mitochondrial function. Proceedings of the National Academy of Sciences of the United States of America. 2007; 104:15560–15565. [PubMed: 17878306]

Elrod JW, Molkentin JD. Physiologic functions of cyclophilin D and the mitochondrial permeability transition pore. Circulation journal: official journal of the Japanese Circulation Society. 2013; 77:1111–1122. [PubMed: 23538482]

Elrod JW, Wong R, Mishra S, Vagnozzi RJ, Sakthievel B, Goonasekera SA, Karch J, Gabel S, Farber J, Force T, et al. Cyclophilin D controls mitochondrial pore-dependent Ca(2+) exchange, metabolic flexibility, and propensity for heart failure in mice. J Clin Invest. 2010; 120:3680–3687. [PubMed: 20890047]

Fan J, Ye J, Kamphorst JJ, Shlomi T, Thompson CB, Rabinowitz JD. Quantitative flux analysis reveals folate-dependent NADPH production. Nature. 2014; 510:298–302. [PubMed: 24805240]

Fieni F, Lee SB, Jan YN, Kirichok Y. Activity of the mitochondrial calcium uniporter varies greatly between tissues. Nature communications. 2012; 3:1317.

Foo RS, Mani K, Kitsis RN. Death begets failure in the heart. J Clin Invest. 2005; 115:565–571. [PubMed: 15765138]

Frezza C, Cipolat S, Scorrano L. Organelle isolation: functional mitochondria from mouse liver, muscle and cultured fibroblasts. Nature protocols. 2007; 2:287–295. [PubMed: 17406588]

Gao E, Lei YH, Shang X, Huang ZM, Zuo L, Boucher M, Fan Q, Chuprun JK, Ma XL, Koch WJ. A novel and efficient model of coronary artery ligation and myocardial infarction in the mouse. Circulation research. 2010; 107:1445–1453. [PubMed: 20966393]

Glancy B, Balaban RS. Role of mitochondrial Ca2+ in the regulation of cellular energetics. Biochemistry. 2012; 51:2959–2973. [PubMed: 22443365]

Hoppe UC. Mitochondrial calcium channels. FEBS Lett. 2010; 584:1975–1981. [PubMed: 20388514]

Howell WH, Duke WW. Experiments on the isolated mammalian heart to show the relation of the inorganic salts to the action of the accelerator and inhibitory nerves. The Journal of physiology. 1906; 35:131–150. [PubMed: 16992867]

Huang YC, Colman RF. Location of the coenzyme binding site in the porcine mitochondrial NADP-dependent isocitrate dehydrogenase. The Journal of biological chemistry. 2005; 280:30349–30353. [PubMed: 15975917]

Jain M, Nilsson R, Sharma S, Madhusudhan N, Kitami T, Souza AL, Kafri R, Kirschner MW, Clish CB, Mootha VK. Metabolite profiling identifies a key role for glycine in rapid cancer cell proliferation. Science (New York, N Y. 2012; 336:1040–1044.

Jiang D, Zhao L, Clapham DE. Genome-wide RNAi screen identifies Letm1 as a mitochondrial Ca2+/H+ antiporter. Science (New York, N Y. 2009; 326:144–147.

Kirichok Y, Krapivinsky G, Clapham DE. The mitochondrial calcium uniporter is a highly selective ion channel. Nature. 2004; 427:360–364. [PubMed: 14737170]

Mallilankaraman K, Doonan P, Cardenas C, Chandramoorthy HC, Muller M, Miller R, Hoffman NE, Gandhirajan RK, Molgo J, Birnbaum MJ, et al. MICU1 is an essential gatekeeper for MCU-mediated mitochondrial Ca(2+) uptake that regulates cell survival. Cell. 2012; 151:630–644. [PubMed: 23101630]

McCormack JG, England PJ. Ruthenium Red inhibits the activation of pyruvate dehydrogenase caused by positive inotropic agents in the perfused rat heart. The Biochemical journal. 1983; 214:581–585. [PubMed: 6193784]

Michels G, Khan IF, Endres-Becker J, Rottlaender D, Herzig S, Ruhparwar A, Wahlers T, Hoppe UC. Regulation of the human cardiac mitochondrial Ca2+ uptake by 2 different voltage-gated Ca2+ channels. Circulation. 2009; 119:2435–2443. [PubMed: 19398664]

Moore CL. Specific inhibition of mitochondrial Ca++ transport by ruthenium red. Biochemical and biophysical research communications. 1971; 42:298–305. [PubMed: 4250976]

Oka T, Maillet M, Watt AJ, Schwartz RJ, Aronow BJ, Duncan SA, Molkentin JD. Cardiac-specific deletion of Gata4 reveals its requirement for hypertrophy, compensation, and myocyte viability. Circulation research. 2006; 98:837–845. [PubMed: 16514068]

Palmieri EM, Spera I, Menga A, Infantino V, Porcelli V, Iacobazzi V, Pierri CL, Hooper DC, Palmieri F, Castegna A. Acetylation of human mitochondrial citrate carrier modulates mitochondrial citrate/malate exchange activity to sustain NADPH production during macrophage activation. Biochim Biophys Acta. 2015

Palty R, Silverman WF, Hershfinkel M, Caporale T, Sensi SL, Parnis J, Nolte C, Fishman D, Shoshan-Barmatz V, Herrmann S, et al. NCLX is an essential component of mitochondrial Na+/Ca2+ exchange. Proceedings of the National Academy of Sciences of the United States of America. 2010; 107:436–441. [PubMed: 20018762]

Pan X, Liu J, Nguyen T, Liu C, Sun J, Teng Y, Fergusson MM, Rovira II, Allen M, Springer DA, et al. The physiological role of mitochondrial calcium revealed by mice lacking the mitochondrial calcium uniporter. Nature cell biology. 2013; 15:1464–1472. [PubMed: 24212091]

Piot C, Croisille P, Staat P, Thibault H, Rioufol G, Mewton N, Elbelghiti R, Cung TT, Bonnefoy E, Angoulvant D, et al. Effect of cyclosporine on reperfusion injury in acute myocardial infarction. The New England journal of medicine. 2008; 359:473–481. [PubMed: 18669426]

Rasola A, Bernardi P. Mitochondrial permeability transition in Ca(2+)-dependent apoptosis and necrosis. Cell calcium. 2011; 50:222–233. [PubMed: 21601280]

Rizzuto R, Pinton P, Carrington W, Fay FS, Fogarty KE, Lifshitz LM, Tuft RA, Pozzan T. Close contacts with the endoplasmic reticulum as determinants of mitochondrial Ca2+ responses. Science (New York, N Y. 1998; 280:1763–1766.

Sottocasa G, Sandri G, Panfili E, De Bernard B, Gazzotti P, Vasington FD, Carafoli E. Isolation of a soluble Ca 2+ binding glycoprotein from ox liver mitochondria. Biochemical and biophysical research communications. 1972; 47:808–813. [PubMed: 4260315]

Unitt JF, McCormack JG, Reid D, MacLachlan LK, England PJ. Direct evidence for a role of intramitochondrial Ca2+ in the regulation of oxidative phosphorylation in the stimulated rat heart. Studies using 31P n.m.r. and ruthenium red. The Biochemical journal. 1989; 262:293–301. [PubMed: 2479373]

Williams GS, Boyman L, Chikando AC, Khairallah RJ, Lederer WJ. Mitochondrial calcium uptake. Proceedings of the National Academy of Sciences of the United States of America. 2013; 110:10479–10486. [PubMed: 23759742]

Williams GS, Boyman L, Lederer WJ. Mitochondrial calcium and the regulation of metabolism in the heart. J Mol Cell Cardiol. 2015; 78:35–45. [PubMed: 25450609]

Wu Y, Rasmussen TP, Koval OM, Joiner ML, Hall DD, Chen B, Luczak ED, Wang Q, Rokita AG, Wehrens XH, et al. The mitochondrial uniporter controls fight or flight heart rate increases. Nature communications. 2015; 6:6081.

Yang L, Luo H, Vinay P, Wu J. Molecular cloning of the cDNA of mouse mitochondrial NADP-dependent isocitrate dehydrogenase and the expression of the gene during lymphocyte activation. Journal of cellular biochemistry. 1996; 60:400–410. [PubMed: 8867815]

Zhang SZ, Gao Q, Cao CM, Bruce IC, Xia Q. Involvement of the mitochondrial calcium uniporter in cardioprotection by ischemic preconditioning. Life sciences. 2006; 78:738–745. [PubMed: 16150463]

Zhao Q, Wang S, Li Y, Wang P, Li S, Guo Y, Yao R. The role of the mitochondrial calcium uniporter in cerebral ischemia/reperfusion injury in rats involves regulation of mitochondrial energy metabolism. Molecular medicine reports. 2013; 7:1073–1080. [PubMed: 23426506]

Zhou YY, Wang SQ, Zhu WZ, Chruscinski A, Kobilka BK, Ziman B, Wang S, Lakatta EG, Cheng H, Xiao RP. Culture and adenoviral infection of adult mouse cardiac myocytes: methods for cellular genetic physiology. Am J Physiol Heart Circ Physiol. 2000; 279:H429–436. [PubMed: 10899083]

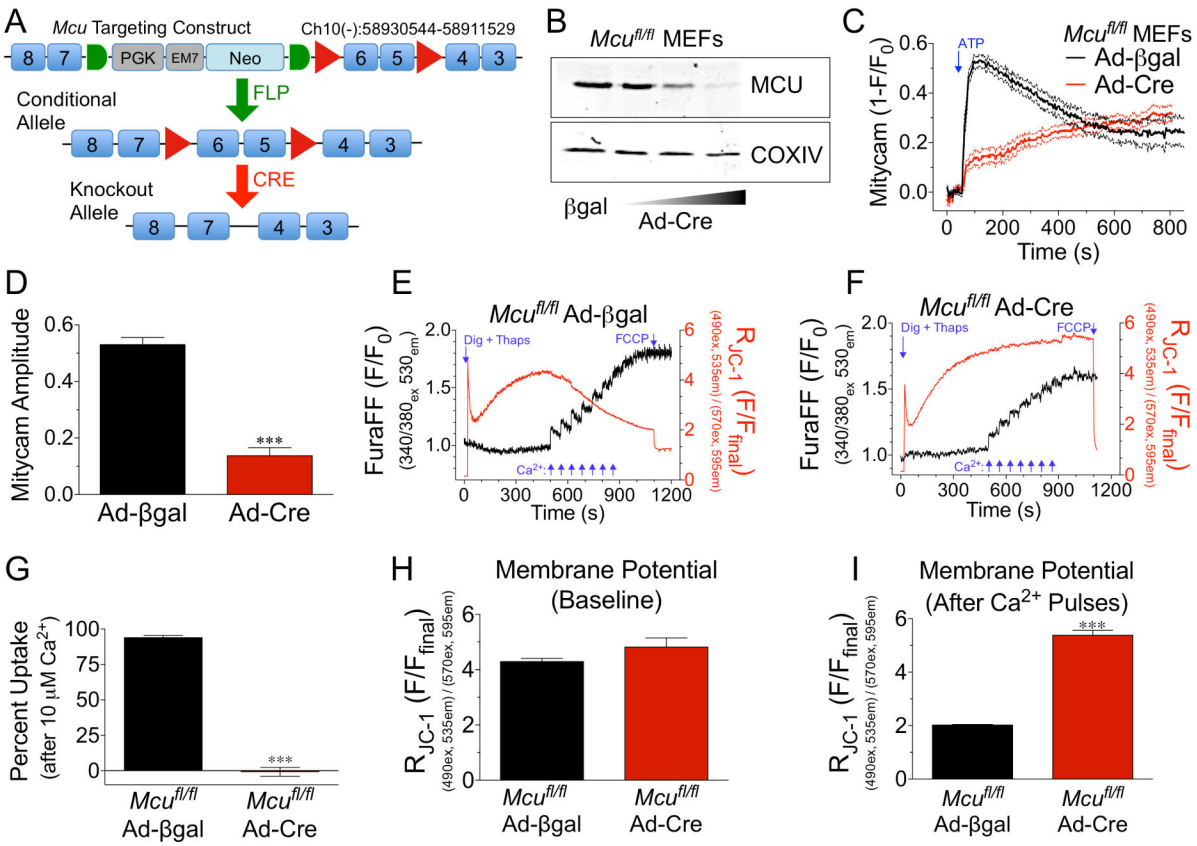

Figure 1. Generation of a conditional Mcu knockout mouse model and confirmation of functionality

A) Schematic of *Mcu* targeting construct. LoxP sites (red triangles) flank exons 5-6. A neomycin (Neo) selection cassette is flanked by FRT sites (green half-circles). Mutant mice were crossed with ROSA26-FLPe mice for removal of Neo. Floxed mice (conditional allele) were crossed with cardiomyocyte-specific Cre-recombinase driver lines resulting in deletion of *Mcu*. **B)** Mouse embryonic fibroblasts (MEFs) were isolated from $Mcu^{fl/fl}$ mice at E13.5. MEFs were infected with adenovirus expressing Cre-recombinase (Ad-Cre) or the experimental control β-galactosidase (Ad-βgal). 6d post infection with Ad-Cre cells were lysed and MCU protein expression examined by western blot. COXIV was used as a mitochondrial loading control. **C)** $Mcu^{fl/fl}$ MEFs were treated with Ad-Cre or Ad-βgal and subsequently infected with Adeno encoding mitycam, $_{m}Ca^{2+}$ sensor, 48h prior to imaging. Baseline was recorded and a single pulse of 1-mM ATP was delivered to liberate $_{i}Ca^{2+}$ stores. Signal means shown as solid lines with dashed lines displaying +/− SEM. **D)** $_{m}Ca^{2+}$ amplitude (peak intensity immediately after ATP – baseline). **E)** $Mcu^{fl/fl}$ MEFs were treated with Ad-βgal and loaded with the Ca^{2+} sensor (Fura-FF) and the Δψ sensor (JC-1) permeabilized with digitonin and treated with thapsigargin (SERCA inhibitor) for simultaneous ratiometric monitoring during repetitive additions of 5-μM Ca^{2+} (blue arrows). FCCP was used as a control to collapse Δψ at the conclusion of each experiment. **F)** $Mcu^{fl/fl}$ MEFs were treated with Ad-Cre and subjected to identical experimental conditions. **G)**

Percent $_{m}Ca^{2+}$ uptake vs. Ad-βgal control cells following 10-μM Ca^{2+} (2^{nd} pulse). **H)** JC-1 derived Δψ prior to Ca^{2+} additions. **I)** JC-1 derived Δψ following 7 pulses of 5-μM Ca^{2+}.

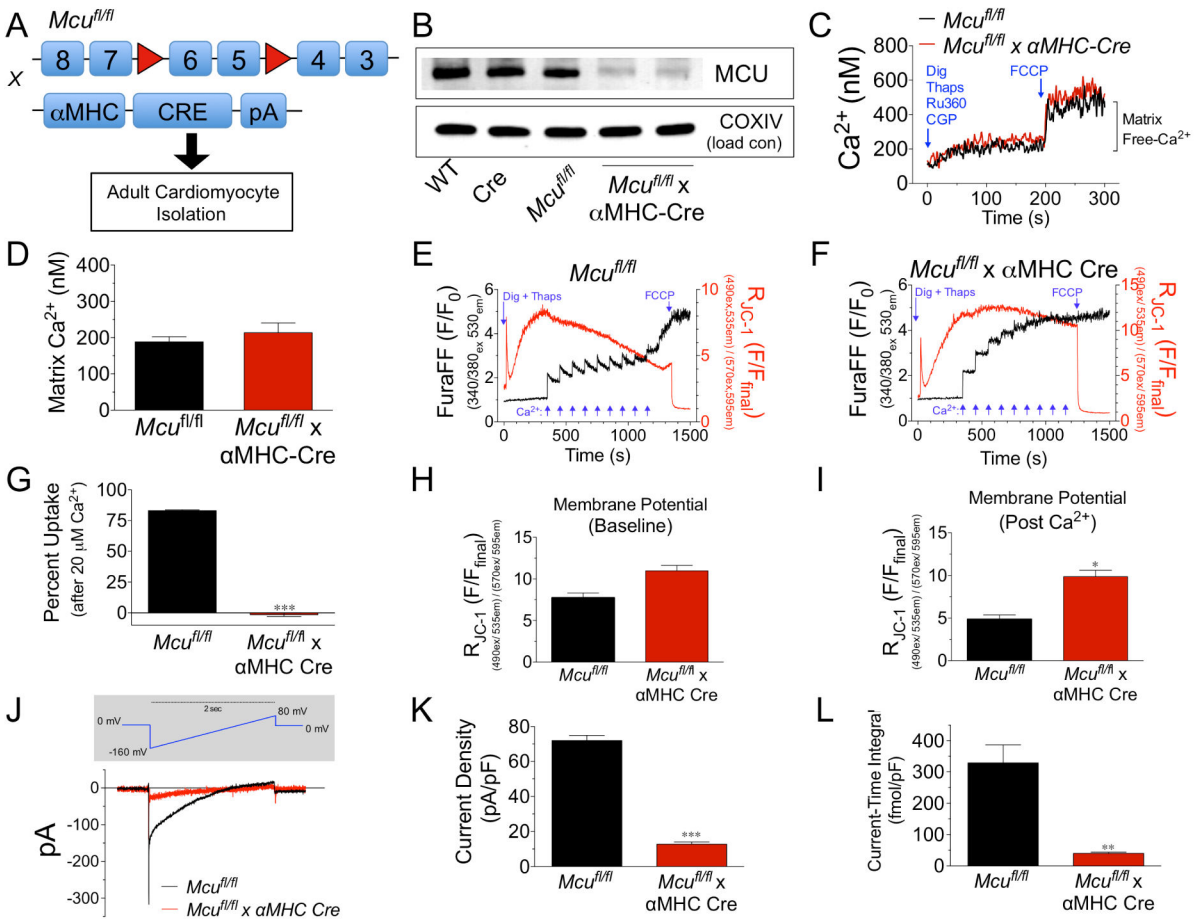

Figure 2. Biophysical characterization of Mcu KO ACMs

A) *Mcu*$^{fl/fl}$ mice were crossed with αMHC-Cre mice and ACMs were isolated from hearts of adult mice. **B)** ACMs were isolated from: wild-type (WT), αMHC-Cre (Cre), *Mcu*$^{fl/fl}$, *and* *Mcu*$^{fl/fl}$ x Cre. Samples were lysed and immunobloted for MCU protein expression and the mitochondrial loading control COXIV. **C)** ACMs were loaded with the Ca^{2+} sensor Fura-2. The sarcolemma was permeabilized with digitonin in the presence of thapsigargin (SERCA inhibitor), CGP-37157 (mNCX inhibitor) and Ru360 (MCU inhibitor). Ca^{2+} levels were recorded and upon reaching a stable baseline, free $_{m}Ca^{2+}$ was released from the mitochondrial matrix with FCCP. **D)** Quantification of matrix Ca^{2+} content after Fura calibration. **E–F)** *Mcu*$^{fl/fl}$ *or* *Mcu*$^{fl/fl}$ x αMHC-Cre ACMs were loaded with the Ca^{2+} sensor (Fura-FF) and the Δψ sensor (JC-1) permeabilized with digitonin and treated with thapsigargin (SERCA inhibitor) for simultaneous ratiometric monitoring during repetitive additions of 10-μM Ca^{2+} (blue arrows). FCCP was used as a control to collapse Δψ at the conclusion of each experiment. **G)** Percent $_{m}Ca^{2+}$ uptake vs. *Mcu*$^{fl/fl}$ following the addition of 20- μM Ca^{2+}. **H–I)** JC-1 quantified Δψ at baseline and post-Ca^{2+} pulses. **J)** Mitochondria were isolated from ACMs and mitoplasts were prepared for recording of MCU current (iMCU). Voltage ramping protocol (above in grey shaded area) and mean current recordings. **K)** Current density measured in picoamperes per picofarad (pA/pF). **L)** Current-time integral measurements, femtomole per picofarad (fmol/pF). *(Minimum of 3 independent*

*experiments for all quantified data, all data shown as mean +/− SEM, *p<0.05, ***p<0.001)*

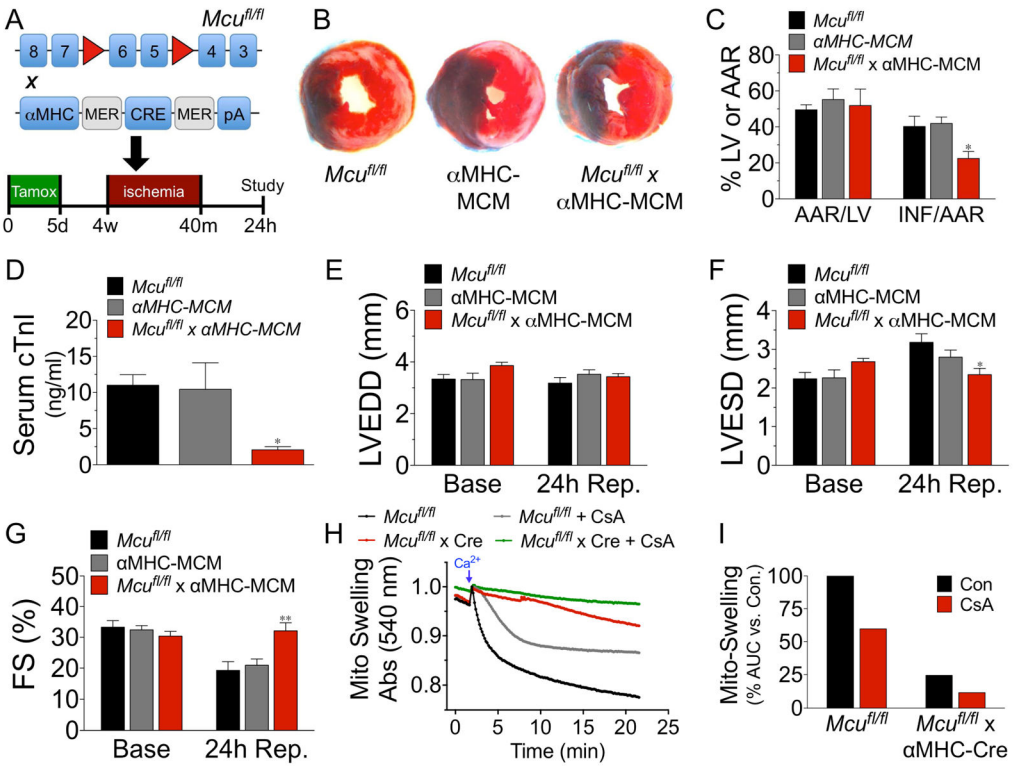

Figure 3. Genetic ablation of Mcu protects against myocardial IR-injury

A) *Mcu*$^{fl/fl}$, αMHC-Mer- Cre-Mer (αMHC MCM) and *Mcu*$^{fl/fl}$ x αMHC-Mer-Cre-Mer mice were treated with tamoxifen (40 mg/kg/day) for 5d to induce cardiomyocyte-restricted Cre expression and allowed to rest for 3wk prior to 40m of ischemia and 24h reperfusion. **B)** Representative mid-ventricular cross sections of TTC stained hearts. (Evan's Blue stained area = non-ischemic zone; remaining area = area-at-risk; white area = infracted tissue; red area = viable myocardium.) **C)** Planimetery analysis of infarct size by quantifying Evan's blue dye excluded area = area-at-risk (AAR), left ventricle (LV) area and non-TTC stained area = infarct (INF). **D)** 24h after reperfusion serum was collected and cardiac troponin-I (cTnI) was measured by ELISA. **E–G)** Mice were analyzed by echocardiography and measurements of LV end-diastolic diameter (LVEDD), LV end-systolic diameter (LVESD), and percent fractional shortening (FS%) were acquired. **H)** Mitochondria were isolated from hearts of adult mice and changes in swelling (decreased absorbance at 540 nm = increase in volume) were assessed +/− 2-μM CsA. Swelling was initiated by injection of 500-μM Ca^{2+}. **I)** Changes in swelling quantified by measuring the area-under-the-curve (AUC) and correcting to control. *(All in vivo experiments minimum of n=7 for all groups; data shown as mean +/− SEM, *p<0.05, **p<0.01)*

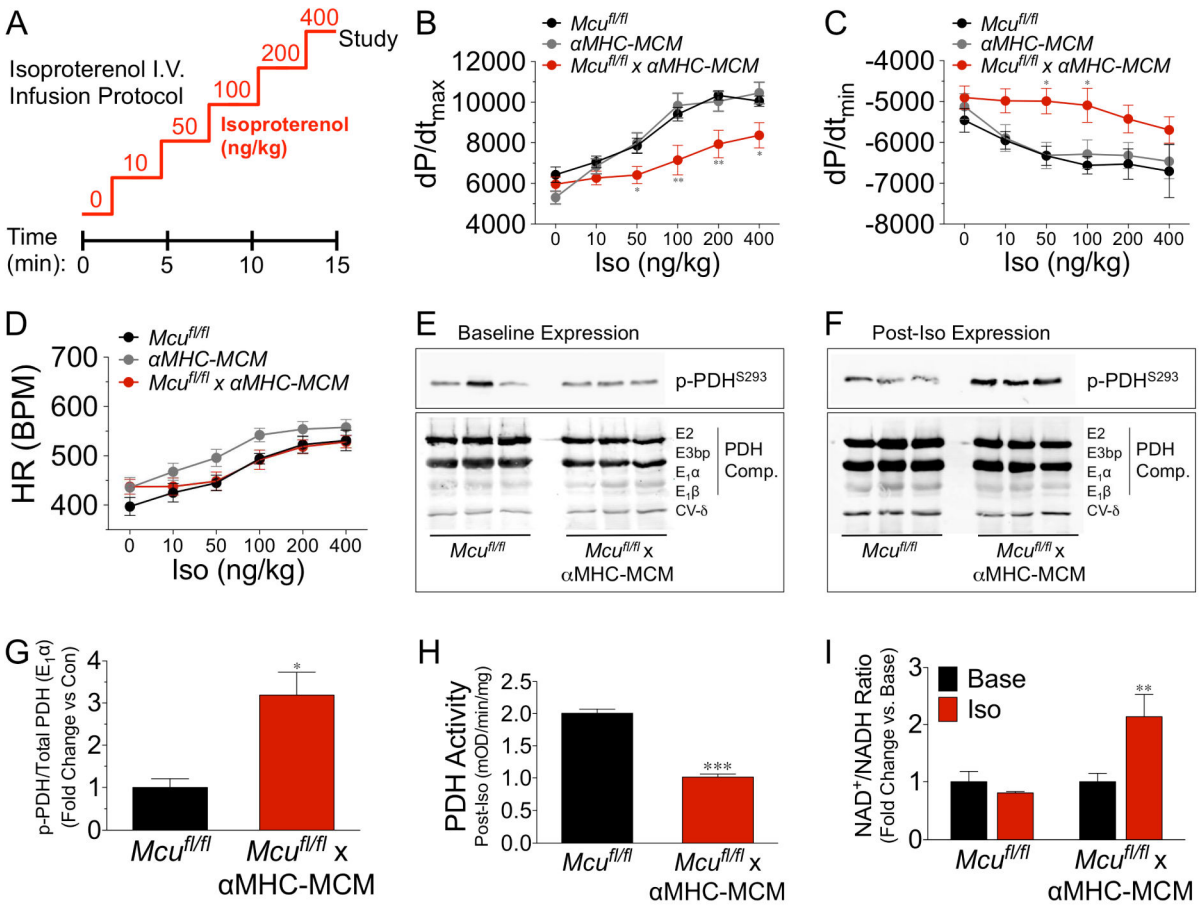

Figure 4. $_{m}Ca^{2+}$ uptake is required for *β-adrenergic-mediated increases in contractility and bioenergetic responsiveness*

A) Mice in all groups received tamoxifen (40 mg/kg/day) for 5d and 1wk later were subjected to an isoproterenol (Iso) infusion protocol (0.1–10 ng/ml) over 15 min. **B–D)** Invasive hemodynamic analysis of dp/dt_{max}, dp/dt_{min}, and heart rate (HR) during Iso infusion (min. n=7/group). **E)** Baseline expression analysis of pyruvate dehydrogenase (PDH) phosphorylation at S293 of the $E_1\alpha$ subunit, and total PDH expression (subunits E2, E3bp, $E_1\alpha$, E1β). ETC Complex V-subunit δ was used as a loading control. **F**) Hearts were freeze-clamped at the conclusion of Iso infusion protocol and western blot examination of PDH phosphorylation at S293 of the $E_1\alpha$ subunit, and total PDH expression (subunits E2, E3bp, $E_1\alpha$, E1β) was performed. **G)** Fold change in PDH phosphorylation vs. control. Band density analysis calculated as $p\text{-}PDH^{S293}$/total PDH ($E_1\alpha$). **H)** PDH activity of samples from hearts during Iso administration, expressed as mOD/min/mg of tissue. **I)** Cardiac NAD^+/NADH ratio following Iso infusion, data expressed as fold-change vs. baseline. *(All data shown as mean +/− SEM, *p<0.05, **p<0.01, ***p<0.001)*

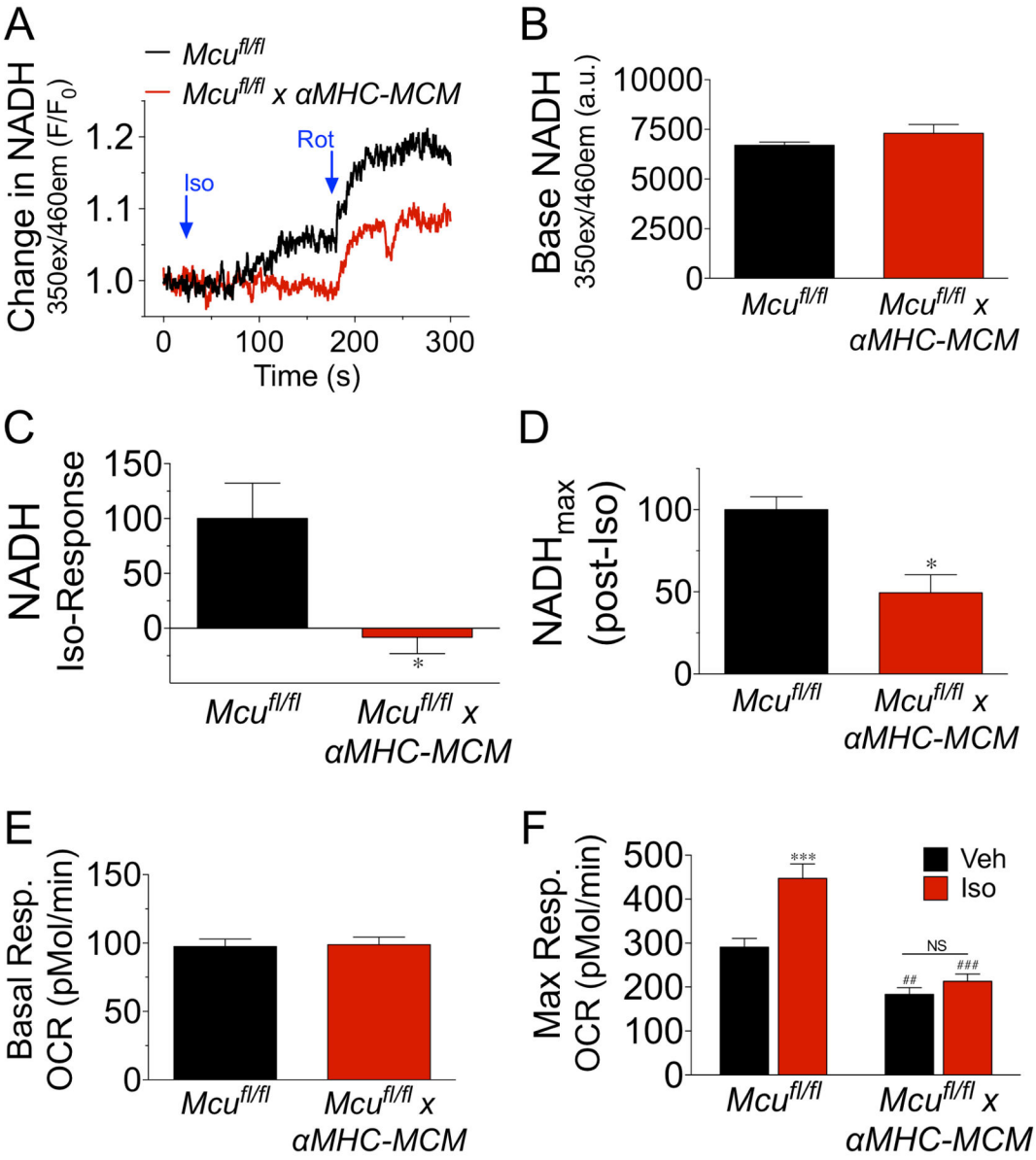

Figure 5. Mcu is necessary for β-adrenergic increases in mitochondrial energetics

ACMs were isolated from *Mcu*$^{fl/fl}$ *and Mcu*$^{fl/fl}$ x αMHC-MCM hearts 1wk post tamoxifen treatment. **A**) ACMs were monitored spectrofluorometrically for changes in NADH autoflourescence after treatment with isoproterenol (Iso, 10-μM) followed by the addition of rotenone (Rot, 2-μM). Mean NADH recording from 3 independent experiments. **B**) Baseline NADH levels calculated as fluorescent intensity. **C**) Percent change in NADH levels following Iso treatment, corrected to *Mcu*$^{fl/fl}$ ACMs. **D**) NADH fluorescent intensity after treatment with rotenone. Calculated as percent change from baseline to post-rotenone corrected to control ACMs. **E**) Isolated ACMs were assayed for mitochondrial OxPhos function using a Seahorse Bioanalyzer to measure oxygen consumption rates (OCR). Baseline OCR. **F**) ACMs were treated with either vehicle (Veh) or isoproterenol (Iso, 10-

μM) and FCCP was injected to augment maximal OCR. *(All data shown as mean +/− SEM, *p<0.05, ***p<0.001 vs. Mcu$^{fl/fl;}$ $^{\#\#}$p<0.01, $^{\#\#\#}$p<0.001 vs. Veh)*